Jurnal Teknologi, 54(Sains & Kejuruteraan) Jan. 2011: 85–100
© Universiti Teknologi Malaysia

IMPROVEMENT OF LOAD FREQUENCY CONTROL BY USING SELF-TUNING CONTROLLER

M. R. I. SHEIKH[1], M. S. ANOWER[2] & M. G. RABBANI[3]

Abstract. Since a Superconducting Magnetic Energy Storage (SMES) unit with a self-commutated converter is capable of controlling both the active and reactive powers simultaneously and quickly, increasing attention has been focused recently on power system stabilization by SMES control. This paper presents a novel control method of SMES with a self-tuned Fuzzy Proportional Integral (FPI) controller associated with the Automatic Generation Control (AGC) for improving Load Frequency Control (LFC) in a single area power system. Boiler dynamics and nonlinearities such as governor dead band (DB) and generator rate constraints (GRC) are considered in the developed comprehensive mathematical model of a single area isolated power system. The effects of the self-tuning configuration of FPI controller in AGC on SMES control is compared with that of fixed gain PI controlled AGC. It is seen that with addition of FPI controller, SMES can perform a more effective primary frequency control for single area power system.

Keywords: Load frequency control; single area power system; automatic generation control; superconducting magnetic energy storage unit; fuzzy proportional integral controller

1.0 INTRODUCTION

Automatic generation control is a very important subject in power system operation for supplying sufficient and reliable electric power. This is achieved by AGC. In an interconnected power system, as the load demand varies randomly, the area frequency and tie-line power interchange also vary. The LFC by only a governor control imposes a limit on the degree to which the deviations in frequency and tie-line power exchange can be decreased. However, as the LFC is fundamentally for the problem of an instantaneous mismatch between the generation and demand of active power, the incorporation of a fast-acting energy storage device in the power system can improve the performance under such conditions. To achieve a better performance, many control strategies are proposed in literature [1–3]. But fixed gain controllers based on classical control theories are presently used. They are not sufficient for the case with changing operating point during a daily cycle [1–5] and also not suitable for all operating conditions. Therefore, variable structure controller [6–7] has been proposed for AGC. For designing controllers based on these techniques, the perfect model is required which has to track the state variables and satisfy system constraints. Therefore it is

[1,2&3]EEE Department, Rajshahi University of Engineering & Technology, 6204, Bangladesh
Email: [1]ris_ruet@yahoo.com, [2]engr_js@yahoo.com, [3]rabbaniruet@yahoo.com

difficult to apply these adaptive control techniques to AGC in practical implementations. In multi area power system, if a load variation occurs at any one of the areas in the system, the frequency related with this area is affected first and then that of other areas are also affected from this perturbation through tie-lines. But, in single area power system, the frequency is affected directly from any type of perturbation. When a small load disturbance occurs, power system frequency oscillations continue for a long duration, even in the case with optimized gain of integral controllers. To damp out the oscillations in the shortest possible time, automatic generation control including proposed controlled SMES unit is used.

In this study, with a simple SMES controller, an isolated generator unit connected to a power line or electric bus that operates for different consumers is considered. The effect of boiler system and governor DB and GRC are also included, by which the worst situation of power system can be considered. As load varies, the frequency of the generator unit varies. Frequency transients must be eliminated as rapidly as possible. It is known that most LFC systems include an integral controller. The integrator gain is set to a level that compromise between fast transient recovery and low overshoot in dynamic response of the system [8]. Unfortunately, this type of controller is slow and impossible in account to generating unit non-linearities.

For this, based on a simple SMES controller, a FPI controller is designed in order to retain the frequency to the rated value after the load changes. The basic objective of the FPI controller is to restore balance between the load and generation after the occurrence of a load disturbance. This is met when the control action maintains the frequency and the power interchange at the scheduled values. It is seen that with the addition of the proposed FPI controller to AGC, a simple controller scheme for SMES is sufficient for load frequency control of single area power system.

2.0 MODELLING OF THE POWER SYSTEM FOR AGC WITH SMES UNIT

The single area power system model with the proposed configuration of SMES units is shown in Figure 1. When there is a sudden rise in power demand in a control area, the stored energy is almost immediately released by the SMES through its power conversion system (PCS). As the governor control mechanism starts working to set the power system to the new equilibrium condition, the SMES coil stores back to its nominal energy. Similar is the action when there is a sudden decrease in load demand. Basically, the governor-turbine system is slow reacting compared with the excitation system, which is fast reacting. As a result, fluctuations in terminal voltage can be corrected by the excitation system very quickly. Fluctuations in generated power or frequency are corrected slowly. Since load frequency control is primarily concerned with the real power/frequency behavior, the excitation system model will not be required in the approximated analysis [3]. This important simplification paves the way for constructing the simulation model shown in Figure 1. The modeling and control design

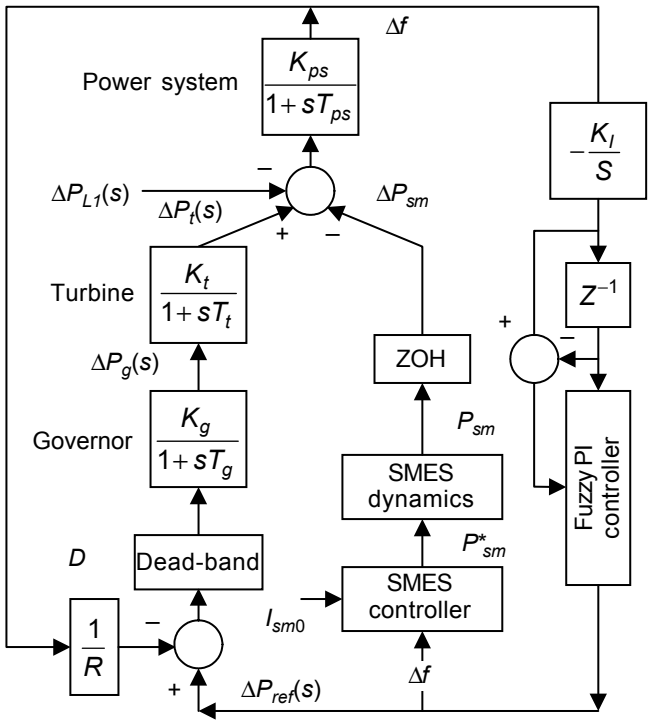

Figure 1 Power system model with SMES

aspects of SMES are separately detailed in the subsequent sections. The presence of zero-hold (ZOH) device in Figure1 implies the discrete mode control character for SMES.

All of the governors have deadband which has significant effect on the dynamic performance of the power system [9]. So effects of governor dead-band are studied in relation to AGC. The limiting value of dead-band is specified as 0.06%. The governor deadband is defined, as the total magnitude of a sustained speed change within which there is no change in valve position. The nonlinearity of hysteresis is expressed as [9]:

$$y = F\left(x, dx/dt\right) \tag{1}$$

For a basic assumption, the variable x is taken as a sinusoidal oscillation

$$x \approx A\sin\omega_0 t \tag{2}$$

where A is the amplitude of oscillation, w_0 is the frequency of oscillation. It has been known that the backlash nonlinearity tends to give continuous sinusoidal oscillation with a natural period of about two seconds [10]. $F(x, dx/dt)$ function can be evaluated as a Fourier series as follows [9]:

$$F(x,\dot{x}) = F^0 + N_1 x + \frac{N_2}{\omega_0}\dot{x} + \ldots \tag{3}$$

Since the backlash nonlinearity is a symmetrical about the origin, the constant term F^0 in the Fourier series is zero [11]. So from equations (3)

$$F(x,\dot{x}) = N_1 x + \frac{N_2}{\omega_0}\dot{x} = Dx \tag{4}$$

where D denotes the deadband [10,11]. Therefore, the describing function incorporating the governor deadband nonlinearity for single area power system is expressed as nonlinear differential equations [12].

Also in practical steam turbine, due to thermodynamic and mathematical constraints, there is a limit to the rate at which its output power (dP_t/dt) can be changed. This limit is referred to as generation rate constraint (GRC). In practice, there exists a maximum limit on the rate of change in the generating power of a steam plant. In the presence of GRC, the dynamic responses of the system experience larger overshoots and longer settling time compared to the case without considering the GRC. Hence, if the load changes are too fast under transient conditions, then system nonlinearities will prevent its achievement. Moreover, if the parameters of the controller are not chosen properly, the system may become unstable. Thus, the GRC is taken into account by adding a limiter to the turbine as shown in Figure 2, with a value of 0.17 p.u. MW/min [11]. This is a typical value up to 3.4 MW/second. All parameters are shown in Table 1.

The modeling equations of the proposed single-area power system are:

$$\Delta\dot{P}_{\text{generation}} = 0.1\text{p.u.MW/min} = 0.0017\text{p.u.MW/sec} = \delta$$

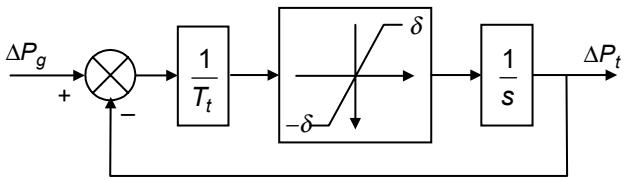

Figure 2 A non-linear turbine model with GRC

$$\Delta\dot{f} = \frac{1}{T_{ps}}\left[K_{ps}\left(\Delta P_t - \Delta P_L - \Delta P_{sm}\right) - \Delta f\right] \tag{5}$$

$$\Delta\dot{P}_t = \frac{1}{T_t}\left(K_t \Delta P_g - \Delta P_t\right) \tag{6}$$

$$\Delta\dot{P}_g = \frac{1}{T_g}\left[K_g.D\left(\Delta P_{ref} - \frac{\Delta f}{R}\right) - \Delta P_g\right] \tag{7}$$

Table 1 **N**ominal parameters of single-area power system

Area capacity	$= P_R$	= 2000 MW
	K_P	= 120 Hz/p.u. MW
	T_P	= 20 sec
	K_G	= 1 Hz/p.u. MW
	T_G	= 0.08 sec
	K_T	=1 Hz/p.u. MW
	T_T	= 0.3 sec
	R	= 2.4 Hz/p.u. MW
	K_I^0	= 0.29 and then varied for FGS controller
	D	= 0.0083 pu. MW/ Hz

$$\Delta \dot{P}_{ref}(t) = -K_I \Delta f(t) \tag{8}$$

3.0 OPTIMIZATION OF THE INTEGRAL GAIN, K_I FOR FIXED GAIN PI CONTROLLER

The tuning of the value of K_I at $K_P = 0$ was achieved using a systematic exhaustive search according to the IAET criterion shown in equation (9).

$$J_{fre} = \int_0^T |\Delta f(t)| t \, dt \tag{9}$$

Considering this performance index (J_{fre}) for the fixed load disturbance, the optimal value of fixed gain K_I is determined for the fixed gain controller. It is found that in the absence of generation rate constraints (GRC) the best-tuned integral gain value is $K_I = 0.29$ & $K_P = 0$ at $J_{fre} = 0.1871$, which is also called the critical value. In the presence of governor dead-band and GRC the gain values of the conventional PI controller are $K_I = 0.27$ & $K_P = 0$ at $J_{fre} = 0.2696$, which is shown in Figure 3.

4.0 CONVENTIONAL PI CONTROL SYSTEM

The general practice in the design of a LFC is to utilize a PI structure. A typical conventional PI control system is shown in Figure 4. This gives adequate system response considering the stability requirements and the performance of its regulating units. In this case the response of the PI controller is not satisfactory enough and large oscillations may occur in the system [13-14]. For that reason, a FPI Controller is designed and implemented in this study.

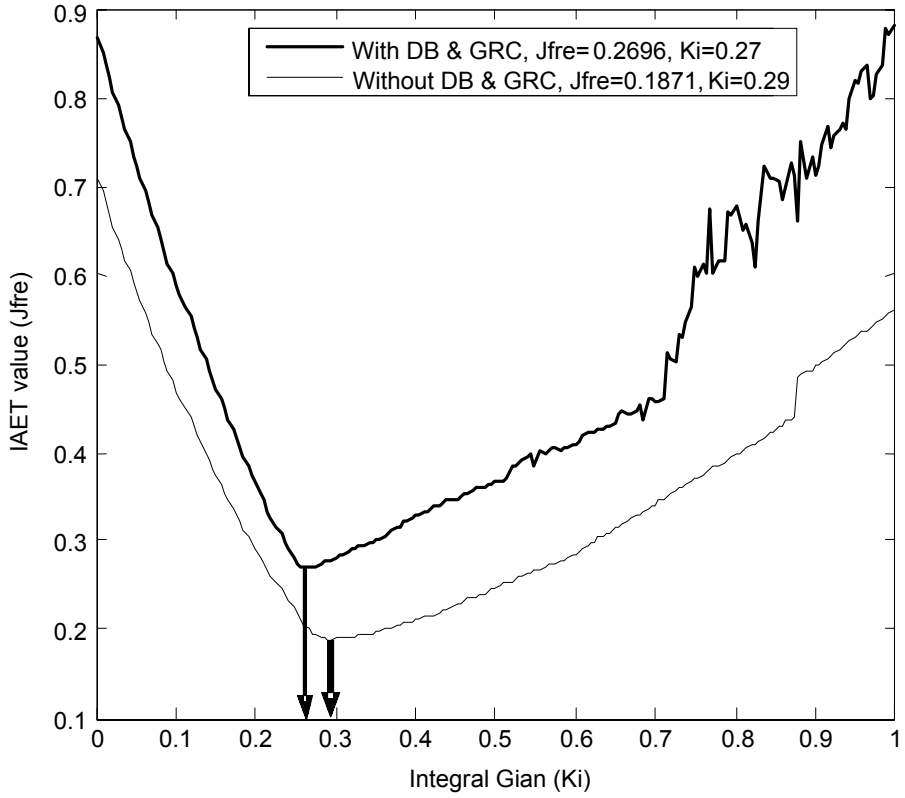

Figure 3 The optimal K_I setting with and without considering DB and GRC

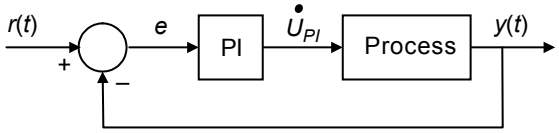

Figure 4 A typical conventional PI controller

5.0 PROPOSED CONTROLLER

Here is the detail description of the proposed controller.

5.1 *Fuzzy PI (FPI) Controller*

A FPI control unit arrangement shown in Figure 5 is used, called the derivative-of-output, which is often desirable, if the reference input contains discontinuity [15]. The discrete-time equivalent expression for PI controller can be expressed as

$$u^*(k) = K_p e^*(k) + K_I T_s \sum_{i=1}^{n} e^*(i) \tag{10}$$

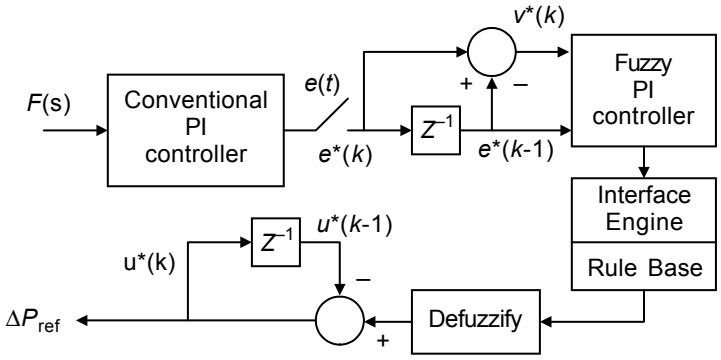

Figure 5 Control block for FPI controller

where, $u(k)$ is the control signal, $e(k)$ is the error between the reference and the process output, T_S is the sampling period for the controller, and

$$\Delta e^*(k) = e^*(k) - e^*(k-1) \tag{11}$$

The incremental control effort at k^{th} instant is given by

$$\Delta u^*(k) = K_p.v^*(k) - K_I.e^*(k-1) \quad \text{and} \quad v^*(k) = \frac{\left[e^*(k) - e^*(k-1)\right]}{T_s} \tag{12}$$

where $\Delta u^*(k)$ is the incremental control effort at k^{th} instant and K_P and K_I are the proportional and integral gains of digital PI controller, respectively. DP_{ref} is the output of the FPI controller.

5.2 *Design Steps for FPI Control Scheme*

Figure 6 shows a schematic representation of a typical clossed loop fuzzy control system. For implimentation of FPI controller, the precise numerical values obtained by

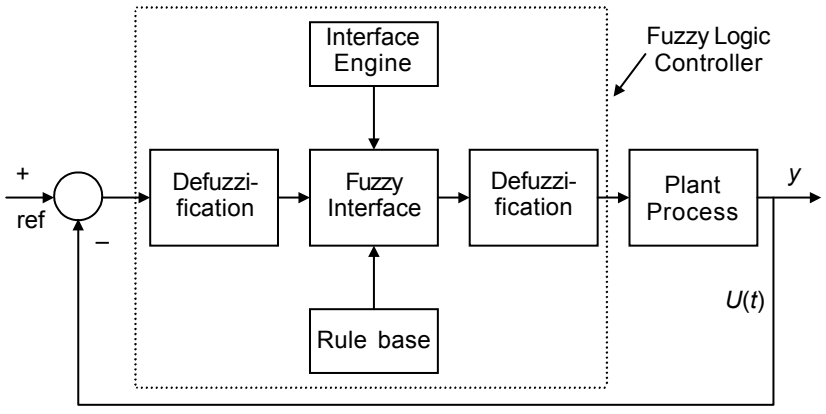

Figure 6 Block diagram of a typical closed-loop fuzzy control system

measurements are converted to membership values of the various linguistic variables. The frequency error signal supplied to the PI controller and then output of the PI controller is fuzzified by the FPI controller. The FPI controller has the two inputs which are defined as:

$$\text{Input 1: error} = e_t = -K_I \int (\Delta f)\, dt \text{ and}$$

$$\text{Input 2: rate of change of error} = c\dot{e}_t = -K_I (\Delta f) \tag{13}$$

where $\Delta f = f_{\text{nom}} - f_t$. The approach taken here is to exploit fuzzy rules and reasoning to generate controller parameters.

The triangular membership functions for the proposed FPI controller of the three variables (e_t, $c\dot{e}_t$, P_{ref}) are shown in Figure 7, where PI controller output (e_t) and change of PI controller output ($c\dot{e}_t$) are used as the inputs of the fuzzy logic controller. Considering these two inputs, the output of FPI controller (ΔP_{ref}) is determined. The use of two input and single output variable makes the design of the controller very straightforward. A membership value for the various linguistic variables is calculated by the rule given by

$$\mu(e_t, c\dot{e}_t) = \min\left[\mu(e_t), \mu(c\dot{e}_t)\right] \tag{14}$$

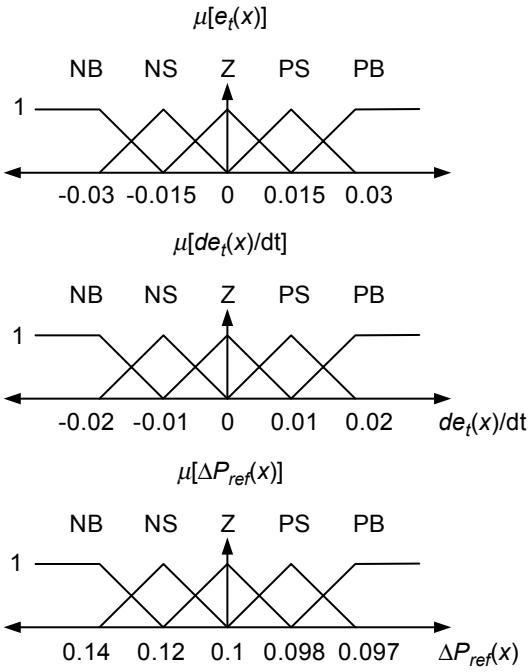

Figure 7 Membership functions for the fuzzy variables

The equation of the triangular membership function used to determine the grade of membership values in this work is as follows:

$$A(x) = \frac{(b - 2|x - a|)}{b} \tag{15}$$

Where $A(x)$ is the value of grade of membership, 'b' is the width and 'a' is the coordinate of the point at which the grade of membership is 1 and x is the value of the input variables. The control rules for the proposed strategy are very straightforward and have been developed from the viewpoint of practical system operation and by trial and error methods. The fuzzy rule base for the FPI controller is shown in Table 2.

Table 2 Fuzzy Rule Base for FPIC

ce \ e	NB	NS	Z	PS	PB
NB	PB	PS	PS	PS	Z
NS	PS	PS	PS	Z	NS
Z	PS	PS	Z	NS	NS
PS	PS	Z	NS	NS	NB
PB	Z	NS	NS	NB	NB

The membership functions, knowledge base and method of defuzzification determine the performance of the FPI controller in a single area power system as shown in equation (15).

$$\Delta P_{ref} = \frac{\sum_{j=1}^{n} \mu_j \mu_j}{\sum_{j=1}^{n} \mu_j} \tag{16}$$

6.0 THE SMES UNIT AND ITS CONTROL STRATEGY

The detail description of the SMES unit and its control strategy has been discussed in this section.

6.1 Overview of SMES unit

The schematic diagram in Figure 8 shows the configuration of a thyristor controlled SMES unit, which is incorporated in the power system for LFC. The converter impresses positive or negative voltage on the superconducting coil by using a cryogenic system

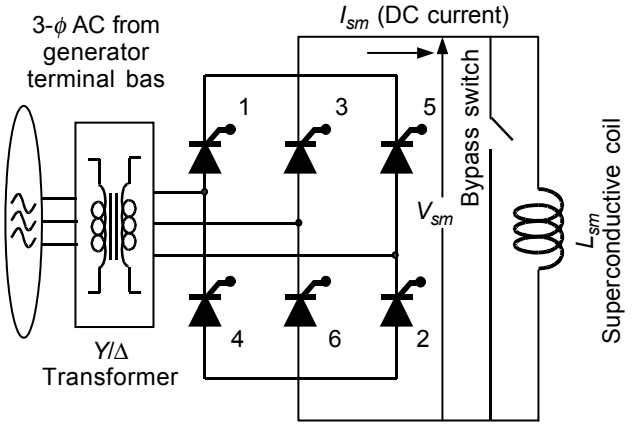

Figure 8 SMES unit with 6-pulse bridge AC/DC thyristor controlled converter

and the power conversion/conditioning system with control and protection functions [16]. Charge and discharge are easily controlled by simply changing the delay angle ±, which controls the sequential firing of the thyristors. If ± is less than 90°, the converter operates in the rectifier mode (charging) and if ± is greater than 90°, the converter operates in the inverter mode (discharging). As a result, power can be absorbed from or released to the power system according to the system requirement. At steady state SMES should not consume any real or reactive power.

For initial charging of the SMES unit, the bridge voltage V_{sm} is held constant at a suitable positive value. The inductor current I_{sm} raises exponentially and magnetic energy W_{sm} is stored in the inductor. When the inductor current reaches its rated value I_{sm0}, it is maintained constant by lowering the voltage across the inductor to zero. The SMES unit is then ready to be coupled to the power system for stabilization.

In actual practice, the inductor current should not be allowed to reach zero to prevent the possibility of discontinuous conduction in the present of large disturbance. To avoid such problems, the lower limit to the inductor current is set to 30% of I_{sm0} [17]. It is desirable to set the rated inductor current I_{sm0} such that the maximum allowable energy absorption equals the maximum allowable energy discharge [18]. This makes the SMES equally effective in damping swings caused by sudden increase as well as decrease in load. Thus, if the lower current limit is chosen at 0.3 I_{sm0}, the upper inductor current limit, based on the equal energy absorption/discharge criterion becomes 1.38 I_{sm0}. When the inductor current reaches either of these limits, the dc voltage has to be brought to zero.

The voltage V_{sm} of the DC side of the converter is expressed by

$$V_{sm} = V_{sm0} \cos\alpha \tag{17}$$

where V_{sm0} is the ideal no-load maximum DC voltage of the bridge.

The current and voltage of superconducting inductor are related as

$$I_{sm} = \frac{1}{L_{sm}} \int_{t_0}^{t} V_{sm} d\tau + I_{sm0} \tag{18}$$

where I_{sm0} is the initial current of the inductor. The real power P_{sm} absorbed or delivered by the SMES unit can be given by

$$P_{sm} = V_{sm} I_{sm} \tag{19}$$

Since the bridge current I_{sm} is not reversible, the bridge output power P_{sm} is uniquely a function of ±, which can be positive or negative depending on V_{sm}. If V_{sm} is positive, power is transferred from the power system to the SMES unit. While if V_{sm} is negative, power is released from the SMES unit. The energy stored in the superconducting inductor is

$$W_{sm} = W_{sm0} + \int_{t_0}^{t} P_{sm} d\tau \tag{20}$$

where $W_{sm0} = \frac{1}{2} L_{sm} I_{sm0}^2$ is the initial energy in the inductor.

6.2 Control System of SMES Unit

Figure 9 outlines the proposed simple control scheme for SMES, which was designed to reduce the instantaneous mismatch between demand and generation. For operating point change due to load changes, FPI controlled AGC including SMES unit is proposed. Firstly DP_{ref} is determined using FPI controller to obtain frequency deviation,

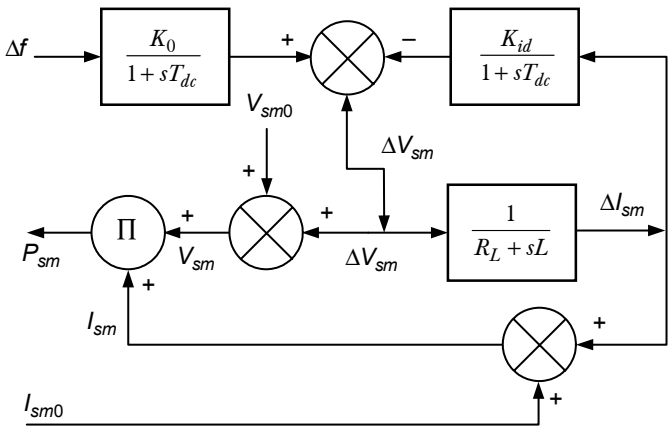

Figure 9 SMES control system

Df and finally this Df is used as the input to the SMES controller. It is desirable to restore the inductor current to its rated value as quickly as possible after a system disturbance, so that the SMES unit can respond properly to any subsequent disturbance. So inductor current deviation is sensed and used as negative feedback signal in the SMES control loop to achieve quick restoration of current and SMES energy level. The parameters of the controller are shown in Table 3.

Table 3

Parameters of SMES controller	
K_0	= 400 kV/p.u. MW
K_{id}	= 2.5 kV/p.u. kA
$I_{sm,max}$	= 6.760482 kA
$I_{sm,min}$	= 1.46967 kA
L_{sm}	= 0.5 Henry
I_{sm0}	= 4.8989 kA
V_{sm0}	= 0 kV
T_{dc}	= 0.026 sec
R_L	= 0.0 W
R_c	= 0.0 W
W_{sm}	= 6 MJ

7.0 SIMULATION RESULTS

To demonstrate the usefulness of the proposed controller, computer simulations were performed using the MATLAB environment under different operating conditions. The system performances with FPI controlled AGC including SMES and optimized fixed gain PI controlled AGC including SMES are shown in Figure 10 through Figure 13. Two cases studies are conducted.

Case I: a step load increase in $\Delta P_L = 0.01$ pu MW is applied in the control area.
Case II: a step load increase in $\Delta P_L = 0.02$ pu MW is applied in the control area.

Form the simulation results it is found that with the addition of SMES unit not only makes the system stable but also the settling time decreases substantially. It is seen from Figures 10 – 13 that the system has more impact when considering DB and GRC compared to the system when it is not considered. When the power system demands the extra power during the first few seconds following the disturbance, energy is supplied from SMES coil by sensing Df signal. The $(K_{id}.\Delta I_{sm})$ term becomes effective only when the inductor current has deviated by a considerable amount. Consequently, the reduction in total energy discharge from the SMES unit does not bring any appreciable deterioration in the frequency and power deviations of the power system. It is interesting

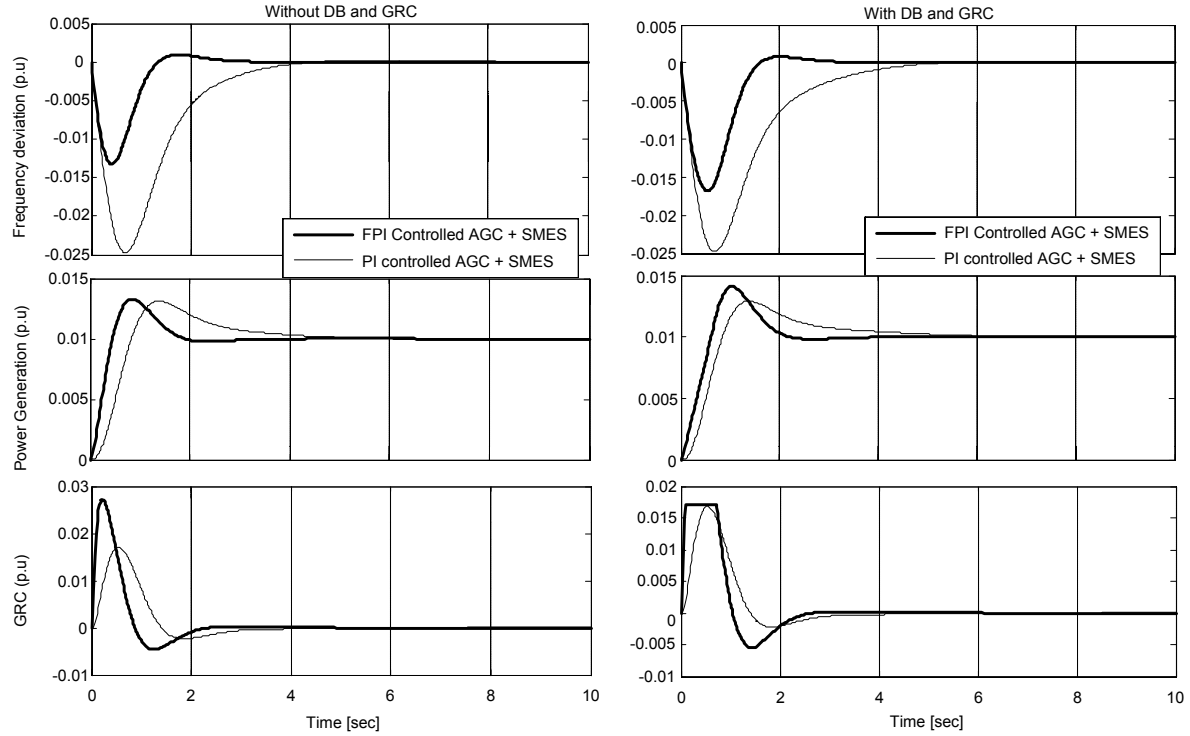

Figure 10 System performances for a step load increase of "P_L= 0.01 p.u MW [**Case I**]

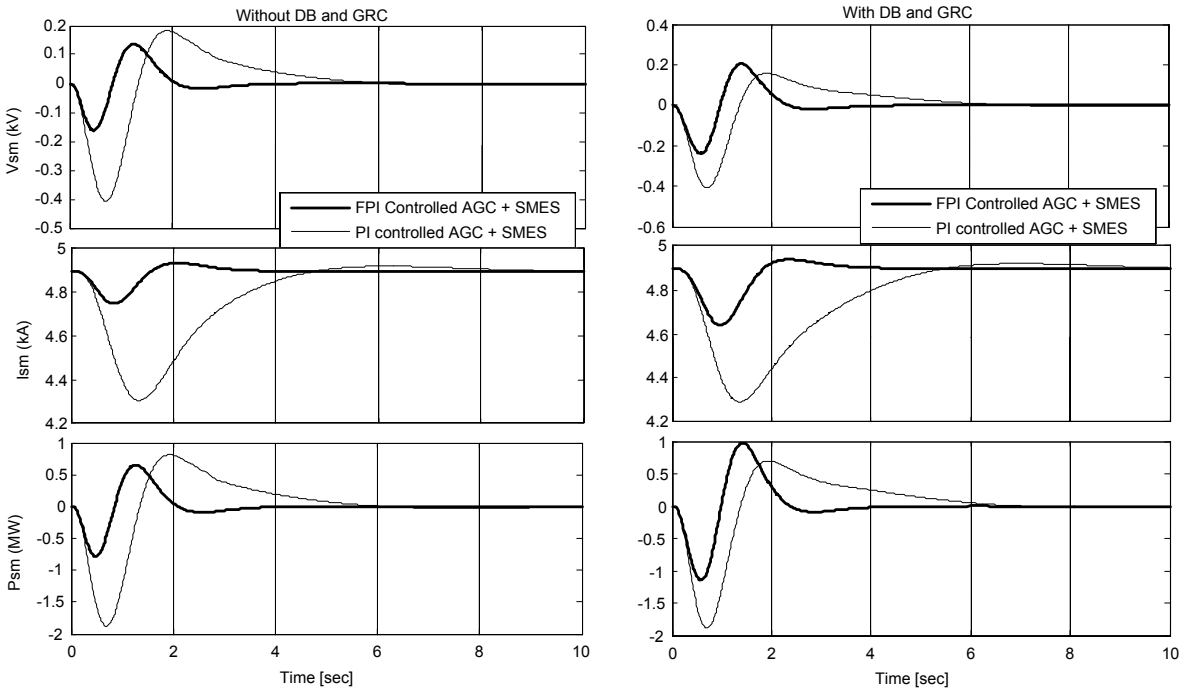

Figure 11 System performances for a step load change of "P_L= 0.01 p.u MW **[Case I]**

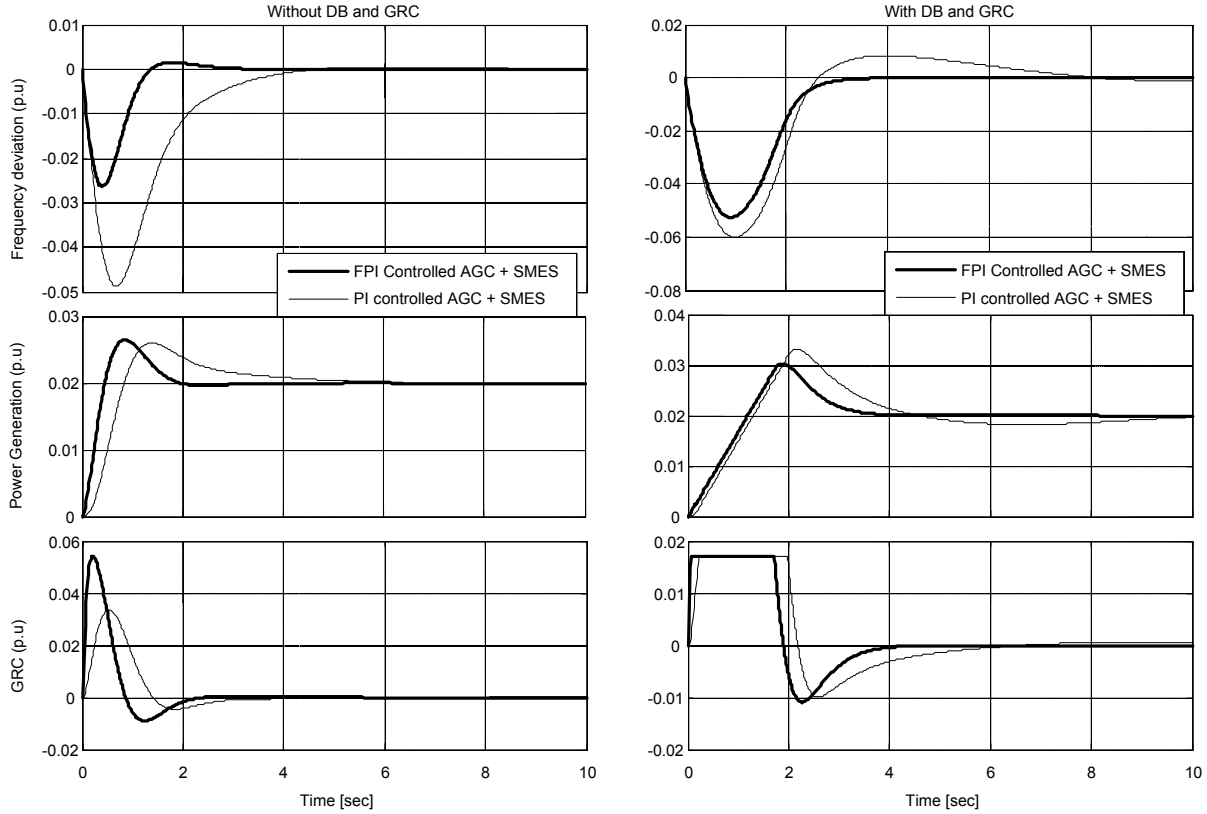

Figure 12 System performances for a step load increase of "P_L= 0.02 p.u MW **[Case II]**

to observe that P_{sm} becomes zero and inductor current (I_{sm}) return back to the rated value quickly after providing appropriate compensation. This enables the SMES unit to respond to a subsequent load disturbance in the power system. It is also observed that the deviation of I_{sm} is less in both the cases when the proposed control system is used. A matter of good satisfaction is that the size of SMES energy capacity is also reduced significantly with the effectively controlled proposed system. Finally it is seen that the damping of the system frequency is not satisfactory for the fixed gain controller. But proposed controlled SMES associated with the FPI controller of AGC significantly improves the system performances.

8.0 CONCLUSIONS

The simulation studies are carried out on a single-area power system considering DB and GRC to investigate the impact of the proposed intelligently controlled SMES for dynamic improvement of LFC. The FPI control approach yields automatic, self-adjusting outputs irrespective of widely varying, imprecise, uncertain off-nominal conditions. The results show that the same control scheme for SMES is very powerful

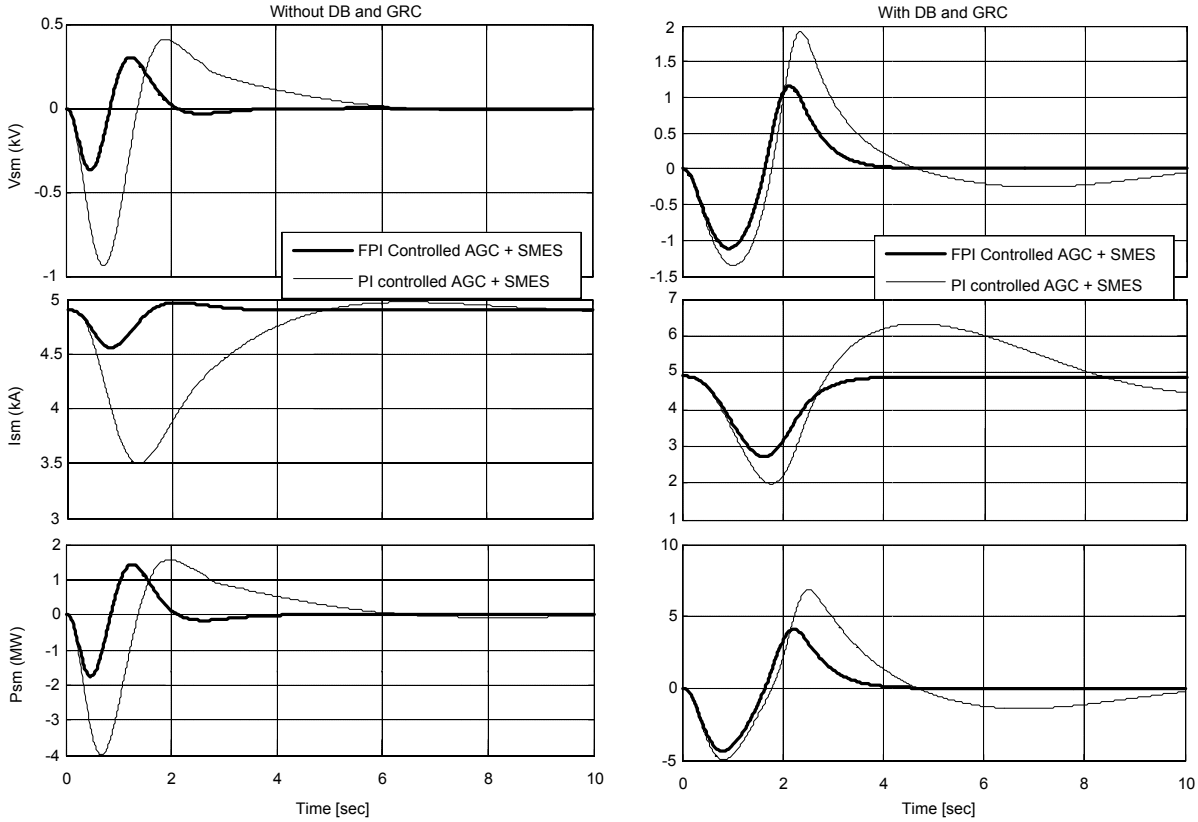

Figure 13 System performances for a step load change of "P_L= 0.02 p.u MW **[Case II]**

in reducing the frequency deviations, in the case when FPI controlled AGC including SMES unit is used compared to optimized fixed gain PI controlled AGC including SMES unit. On line adaptation of FPI controller output associated with SMES makes the proposed intelligent controller more effective and are expected to perform optimally under different operating conditions.

REFERENCES

[1] Nanda, J., B. L. Kavi. 1988. Automatic Generation Control of Interconnected Power System. *IEE Proceedings, Generation, Transmission and Distribution*. 125(5): 385-390.

[2] Nanda, J., A. Mangla, and S. Suri. 2006. Some New Findings on Automatic Generation Control of an Interconnected Hydrothermal System with Conventional Controllers. *IEEE Transactions on Energy Conversion*. 21(1): 187-194.

[3] Mairaj uddin Mufti, Shameem Ahmad Lone, Sheikh Javed Iqbal, Imran Mushtaq. 2007. Improved Load Frequency Control with Superconducting Magnetic Energy Storage in Interconnected Power System. *IEEJ Transaction*. 2: 179-397.

[4] Benjamin, N. N., W. C. Chan. 1978. Multilevel Load-frequency Control of Inter-Connected Power Systems. *IEE Proceedings, Generation, Transmission and Distribution*. 125: 521-526.

[5] Subbaraj, P., and K. Manickavasagam. 2007. Automatic generation control of multi-area power system using fuzzy logic controller. *Euro Trans. of Elec. Power,* Published online in Wiley InterScience, DOI: 10.1002/etep.175.

[6] Benjamin, N. N., W. C. Chan. 1982. Variable Structure Control of Electric Power Generation. *IEEE Transactions on Power Apparatus and System*. 101(2): 376-380.

[7] Sivaramaksishana, A. Y., M. V. Hariharan, and M. C. Srisailam. 1984. Design of Variable Structure Load-Frequency Controller Using Pole Assignment Techniques. *International Journal of Control*. 40(3): 437-498.

[8] Zeynelgil, H. L., A. Demiroren, and N. S. Sengor. 2002. Load Frequency Control for Power System with Reheat Steam Turbine and Governor Deadband Non-linearity by Using Neural Network Controller. *ETEP* 12(3): 179-184.

[9] Tripathy, S. C., G. S. Hope, O. P. Malik. 1982. Optimization of Load-Frequency Control Parameters for Power Systems with Reheat Steam Turbines and Governor Deadband Nonlinearity. *IEE Proc. Pt.C* 129. 1: 10-16.

[10] Beaufays, F., Y. Abdel-Magid, and B. Widrow. 1994. Application of Neural Network to Load-Frequency Control in Power Systems. *Neural Networks*. 7(1): 183-194.

[11] Pan, C. T., and C. M. Lian. 1988. An Adaptive Controller For Power System Load-Frequency Control. *IEEE Transactions on Power System*. 4(1).

[12] Demiroren, A., S. Kent, and T. Giinel. 2002. A Genetic Approach to the Optimization of Automatic Generation Control Parameters for Power Systems. *ETEP*. 12(4): 277-281.

[13] Hossain, M. F., T. Takahashi, M. G. Rabbani, M. R. I. Sheikh, and M. S. Anower. 2006. Fuzzy-Proportional Integral Controller for an AGC in a Single Area Power System. *4th international conference on Electrical & computer Engineering (ICECE)*. 120-123.

[14] Anower, M. S., M. G. Rabbani, M. F. Hossain, M. R. I. Sheikh, and M. Rakibul Islam. 2006. Fuzzy Frequency Controller for an AGC for the Improvement of Power System Dynamics. *4th international conference on Electrical & computer Engineering (ICECE)*. 5-8.

[15] Ambalal V. Patel. 2005. Simplest Fuzzy PI controllers under various Defuzzification Methods. International Journal of Computational Cognition. 3(1). (http://www.Yangsky.com/Yangijcc.comhtm).

[16] IEEE Task Force on Benchmark Models for Digital Simulation of FACTS and Custom–Power Controllers, T&D Committee. Detailed Modeling of Superconducting Magnetic Energy Storage (SMES) System. *IEEE Trans. Power Delivery*. 21(2): 699-710.

[17] Banerjee, S., J. K. Chatterjee, and S. C. Tripathy. 1990. Application of Magnetic Energy Storage Unit as Load Frequency Stabilizer. *IEEE Trans. on Energy Conversion*. 5(1): 46-51.

[18] Ali, M. H., T. Murata, and J. Tamura. 2007. A Fuzzy Logic Controlled Superconducting Magnetic Energy Storage for Transient Stability Augmentation. *IEEE Transaction on Control Systems Technology*. 15(1): 144-150.